Talanta 99 (2012) 737–743

Contents lists available at SciVerse ScienceDirect

Talanta

journal homepage: www.elsevier.com/locate/talanta

Thick-film voltammetric pH-sensors with internal indicator and reference species

Arnaud Emmanuel Musa [a], María Asunción Alonso-Lomillo [b], Francisco Javier del Campo [c], Natalia Abramova [c], Olga Domínguez-Renedo [b], María Julia Arcos-Martínez [b], Jörg Peter Kutter [a,*]

[a] DTU Nanotech—Department of Micro- and Nanotechnology, Technical University of Denmark (DTU), Ørsteds Plads Building 344, 2800 Kongens Lyngby, Denmark
[b] Departamento de Química Analítica, Facultad de Ciencias, Universidad de Burgos, Pza. Misael Bañuelos, 09001 Burgos, Spain
[c] Instituto de Microelectrónica de Barcelona, IMB-CNM (CSIC), Esfera UAB, Campus Universitat Autónoma de Barcelona, 08193 Bellaterra, Barcelona, Spain

ARTICLE INFO

Article history:
Received 23 March 2012
Received in revised form
25 June 2012
Accepted 5 July 2012
Available online 24 July 2012

Keywords:
Voltammetric sensors
Internal reference species
Derivative voltammetry
Disposable sensors
Screen-printing

ABSTRACT

The following paper describes the development of a screen-printed voltammetric pH-sensor based on graphite electrodes incorporating both internal indicator (i.e., phenanthraquinone) and reference species (i.e., dimethylferrocene). The key advantages of this type of system stem from its simplicity, low cost and ease of fabrication. More importantly, as opposed to conventional voltammetric systems where the height of the voltammetric peaks is taken into account to quantify the amount of a species of interest, here, the difference between the peak potential of the indicator species and the peak potential of the reference species is used. Thus, this measurement principle makes the electrochemical system presented here less dependent on the potential of the reference electrode (RE), as is often the case in other electrochemical systems. The developed system displays very promising performances, with a reproducible Super Nernstian response to pH changes and a lifetime of at least nine days.

© 2012 Elsevier B.V. All rights reserved.

1. Introduction

Despite the large success of electrochemical sensors in a number of fields (e.g., clinical, environmental or food industry [1]), a critical issue has restricted their use for certain industrial and biomedical applications: the unavailability of a reliable and durable miniature reference electrode (RE). Miniaturization of electrochemical sensors has often been limited to the working electrode and in many cases a commercial macroscopic RE is still used alongside the miniaturized working electrode [2]. However, within the last 15 years many different promising solutions have been proposed. For instance, among the routes pursued to develop miniaturized REs are thin-film technology [2–6], screen-printing (SP) technology [7–9], conducting polymers [10–15], nanofluidic channels acting as salt bridge [16], a solid crystalline KCl melt [17], polyacrylate microspheres composite [18], and non organic materials [19]. Very good reviews highlighting some of the state-of-the-art microfabricated REs have been published recently [20,21]. However, as agreed by most who have been involved in the development of electrochemical systems, the miniaturization and batch-fabrication of a reliable RE is one of the most difficult challenges left in the field [22]. It is even considered by many as being equal to the quest for the Holy Grail [23].

All the previously mentioned work aimed at developing a stable and reliable RE by solving the endless possible issues stemming from the RE (e.g., complex or expensive fabrication, drift, membrane shrinkage and/or delamination, long conditioning times, etc.).The present article circumvents these challenges using a simple approach and low cost alternative type of electrochemical system featuring a sensing electrode incorporating both sensing and reference species in combination with a quasi-reference electrode (QRE).

The system investigated was intended for pH monitoring and thus featured phenanthraquinone (denoted here as PAQ) as a pH-sensitive moiety (i.e., indicator species) and dimethylferrocene (denoted here as Fc) as a pH-insensitive moiety (i.e., reference species). The redox reactions of PAQ and Fc are shown in Eqs. (1) and (2), respectively.

$$PAQ + 2e^- + 2H^+ \Leftrightarrow PAQH_2 \quad (1)$$

$$Fc^+ + e^- \Leftrightarrow Fc \quad (2)$$

The measurement method used for this type of voltammetric system is based on evaluating pH changes by monitoring the deviation in peak potential of PAQ with respect to Fc. This is a very attractive strategy that allows this type of electrochemical system to theoretically be unaffected by RE potential drift [24,25].

* Corresponding author.
E-mail address: Joerg.Kutter@nanotech.dtu.dk (J.P. Kutter).

0039-9140/$ - see front matter © 2012 Elsevier B.V. All rights reserved.
http://dx.doi.org/10.1016/j.talanta.2012.07.014

In addition, with the voltammetry technique used here, the height of the peak current is not as significant as in typical voltammetric measurements, where this height is used to determine the concentration of a target species. Here, only the location of the peak currents (i.e., the potential) is needed for analysis.

The sensors developed here were produced by screen-printing (SP). Adapted from the microelectronics industry, the thick-film process of SP is one of the most commonly used techniques to deposit coatings in the sub-millimeter range. SP is an inexpensive, simple, versatile and highly reproducible large-scale production technique [26–28]. It involves pressing different pastes or inks through a porous screen to transfer patterns onto a substrate. Originally used on ceramic materials due to their good mechanical, chemical and, especially, thermal properties, SP is today also applied on a broader range of substrates including paper, fabrics and plastics [8,29]. An important application of this technology lies in the fabrication of planar components for miniaturized electrochemical sensors, which have proven their suitability in the biomedical, environmental and industrial fields [30–33]. All these advantages and features attest that SP is one of the most suitable technologies for fast fabrication of low-cost electrochemical voltammetric systems in this work.

To the authors' knowledge, screen-printing of this type of voltammetric pH-sensors has previously only been investigated by Kampouris et al. in 2009 [25]. Inspired by this article and other relevant papers dealing with quinone and ferrocene based electrochemical systems [24,34,35], the presented work intends to pursue the development of low cost voltammetric pH-microsensors. However, here the aim was focused on developing microsensors for a narrower application range (i.e., medical applications), namely, for monitoring pH in physiological samples.

2. Experimental

2.1. Reagents

1,1′-Dimethylferrocene and 9,10-Phenanthrenequinone as well as the reagents used for the electrochemical characterization of the sensors (i.e., KNO_3 and $K_4Fe(CN)_6$) were all of analytical grade and were used as received from Sigma-Aldrich, Denmark, without further purification. Stock solutions were prepared weekly with deionized (DI) water with a minimum resistivity of 18 MΩ cm.

2.2. Materials and instrumentation

2.2.1. Fabrication of the voltammetric sensors

The screen-printed platforms were produced with a *DEK 248* screen-printing machine (*DEK*, UK). Three different polyester *DEK 230* screens with the appropriate stencil patterns were used for printing the relevant layers of the electrochemical systems. The screens were aligned semi-automatically using a *DEK align-4-vision* system.

A manual SP setup was developed for the fabrication of the voltammetric sensors. It was composed of a polymethylmethacrylate (PMMA) platform and frame and a 100 μm thick cyclo olefin polymer (COP) screen structured with the desired patterns by either micromilling [36] or CO_2-laser ablation [37,38].

A SP squeegee (*Speedball Art Product Company*, US) was also used for manual SP of the sensors on top of the platforms. Dust free cellulose polyester wipes (*Sitix IMTEX*, Denmark) were used to gently polish the sensor surfaces.

For the sensor fabrication, graphite (*C10903P14*) and Ag/AgCl (*C2040308D2*) inks were obtained from Gwent, UK. The dielectric material (*242-SB*) was obtained from *Electro-Science Laboratories* (*ESL*), *Inc.*, USA. 500 μm thick PET sheets from *HiFi Industrial Film*, France were utilized as substrate material.

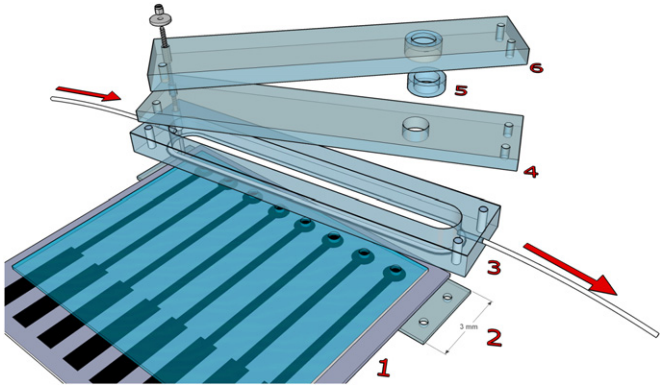

Fig. 1. Microfluidic flow cell for screen-printed electrodes (SPEs): 1–developed chip with SPEs, 2–PMMA bottom part, 3–PDMS chamber with fluidic tubing, 4–PMMA middle part, 5–PDMS o-ring, and 6–PMMA top part (with insertion plug for RE or CE). The test solution flows across the cell as depicted by the arrows.

2.2.2. Micro-fluidic flow cell

In order to reduce sample volumes and facilitate electrochemical characterization of the developed sensors, a fluidic flow-cell (volume of 280 μl) was fabricated (Fig. 1). This cell was composed of PMMA parts (Fig. 1, layers 2, 4 and 6) structured by micromilling, and polydimethylsiloxane (PDMS) parts (Fig. 1, layers 3 and 5) made by replica molding. PMMA sheets (*Nordiskplast*, Denmark) of thicknesses ranging from 1 to 5 mm and PDMS (*Dow Corning*, Denmark) were used for the fabrication of this flow cell.

The PDMS parts were especially designed in order to reversibly seal the fluidic cell on the sensor chip to be tested. For instance, the fluidic chamber part (Fig. 1, layer 3) featured a small ridge (200 μm wide × 100 μm high) at its bottom providing a leak proof sealing with the electrochemical chip. The top part of the fluidic cell featured a plug (Fig. 1, layers 4, 5 and 6) designed to permit the easy introduction of a macro-electrode (i.e., reference or counter electrode) in the fluidic chamber. Moreover, if the use of an additional macro-electrode was not necessary, the top part of the cell could also easily be closed by replacing layers 4, 5 and 6 in Fig. 1 with a simple PMMA lid.

2.3. Characterization apparatus

The surface properties of the sensors were investigated with a *Nikon Eclipse L 200* optical microscope (*Nikon*, Denmark). A stylus profiler (*Dektak 8*, *Bruker AXS*, UK) was also used for determination of the thickness of the different screen-printed layers.

The electrochemical measurements were carried out with a *CH700 series* electrochemical workstation (*CH Instruments*, USA) controlled by a *Windows* based PC. For the measurements, the electrodes developed were used as working electrodes, in combination with a double junction Ag/AgCl (3 M KCl) reference electrode (DJRE, *Metrohm*, Denmark) and a glassy carbon rod as counter electrode (CE).

The electrical properties of the SPEs were investigated by electrical resistance measurements using a *Metex M3850D* digital multimeter (*Metex Instruments*, USA).

2.4. Methods

2.4.1. Fabrication process of the screen-printed sensors

The fabricated chips were composed of semi-automatically screen-printed platforms and consisted of eight electrodes, including four graphite electrodes for the working electrodes (WE) and four Ag/AgCl electrodes for the QREs. The SP process (curing temperature and time) of the different layers of the platforms was carefully optimized [39].

On top of the graphite electrodes, the voltammetric sensors were manually screen-printed for fast fabrication of low cost electrochemical systems. The graphite patterns were cured at 40 °C for 15 min. This low temperature curing process was used in order not to alter the chemicals loaded in the ink via thermal degradation [25]. After curing, the sensors were left overnight at room temperature for further drying. The electrode patterns were then gently polished with a dust free wipe and rinsed with DI water.

Based on the work mentioned above [25], different graphite paste compositions with different weight to weight ratios of electrochemically active components were investigated. Ratios of 1:6 (PAQ or Fc to graphite ink) were first used. Later (see SWV experiments, Section 3.3.2), ratios of 1:3 (PAQ to ink) and 1:6 (Fc to ink) were also investigated. The composition of the electrodes was optimized to obtain voltammetric peaks as clearly resolved as possible.

2.4.2. Electrochemical methods

Electrochemical characterization of the SPEs was carried out by cyclic voltammetry (CV) at a scan rate (υ) ranging from 25 to 500 mV s^{-1}. For the CV experiments, the fabricated sensor was used as WE in combination with a platinum CE, and either a double-junction reference electrode (DJRE) or a fabricated Ag/AgCl quasi-reference electrode.

Square-wave voltammetry (SWV) was performed with a frequency ranging from 10 to 100 Hz, a step potential of 1 mV and an amplitude of 10 mV. Moreover, derivative voltammetry was used to optimize the location of the peak potentials. This method was introduced to precisely determine the peak positions in the square-wave voltammograms by taking the first derivative of the voltammograms [40]. For the SWV experiments, the fabricated sensor was used as working electrode in combination with a platinum CE, and an Ag/AgCl DJRE.

Unless otherwise stated, all potentials are given with respect to the DJRE. All electrochemical experiments were conducted at room temperature (22 ± 2 °C).

3. Results and discussion

3.1. Graphite based sensors

First, to verify the quality of the fabrication technique used, graphite patterns without electroactive species loaded were printed and analyzed.

Analysis of the dimensions of the graphite electrodes by optical microscopy revealed well reproduced printed patterns with an average diameter of 1.23 ± 0.01 mm ($n=3$ samples) which was in good agreement with the diameter of the micro-milled (or laser ablated) holes in the screen (i.e., 1.2 mm). The average thickness of the printed patterns was 64.1 ± 4.5 μm ($n=3$ samples), which revealed the expected shrinkage of the paste caused by the thermal treatment.

Profilometer measurements showed an average surface roughness of 1.3 ± 0.1 μm ($n=3$ samples). This was very close to the roughness values obtained in a comparative study for semi-automatically fabricated SPEs (i.e., 1.62 ± 0.03 μm) [39]. Here, the slightly smoother surface obtained could be attributed to the removal of less non-metallic material during the low temperature curing step and the additional polishing step. As expected, the reproducibility of the manual printing process was lower than what can be achieved with the semi-automatic one, which was highlighted by the higher deviation values.

The electrochemical properties of the printed patterns were then investigated by CV. Typical voltammograms obtained for the manually printed graphite electrodes are shown in Fig. 2A.

The electrodes displayed good voltammograms with polarization curves characteristic for the behavior of a reversible redox couple at the surface of macro-electrodes. Well-defined anodic and cathodic peaks were observed. From voltammograms carried out over a broad range of scan rates (25 to 500 mV s^{-1}), the average peak separation value ΔE_p was typically 150 ± 40 mV whereas the peak current ratio i_p was 1.4 ± 0.2. Those values were very close to the ones obtained for the semi-automatically fabricated SPEs [39] and confirmed that both the curing treatment and the fabrication method used here provided very good results. Moreover, as depicted in Fig. 2B, a linear relationship was obtained when plotting the peak currents versus the square root of the scan rate. This confirmed that a reversible process (i.e., with fast electron transfer and thus a diffusion controlled process) takes place at the surface of the manually printed electrodes.

3.2. Sensors with incorporated electrochemically active species

Sensors incorporating either PAQ or Fc in the graphite paste were fabricated and then characterized.

The cyclic voltammograms of the electrodes incorporating only the PAQ compounds showed a strong anodic peak on the forward scan and a shoulder on the backward scan, thus also

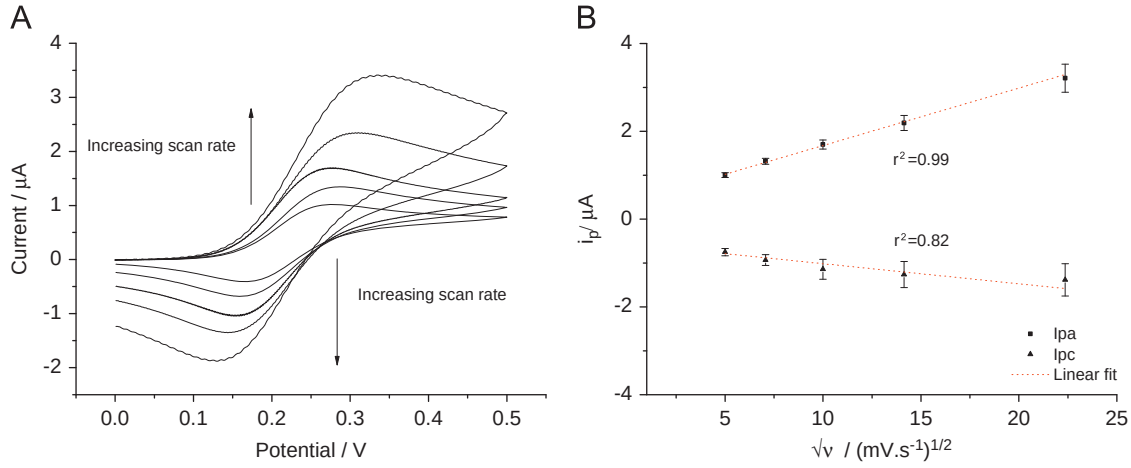

Fig. 2. (A) Overlaid cyclic voltammograms of a manually screen-printed graphite electrode in 1 mM $K_4Fe(CN)_6$ with 0.1 M KNO_3 recorded at varying scan rates (υ from 25 to 500 mV s^{-1}). B. Corresponding plot of the relationship between anodic peak current I_{Pa} (■) and cathodic peak current I_{Pc} (▲) and various scan rate values ($n=3$ samples).

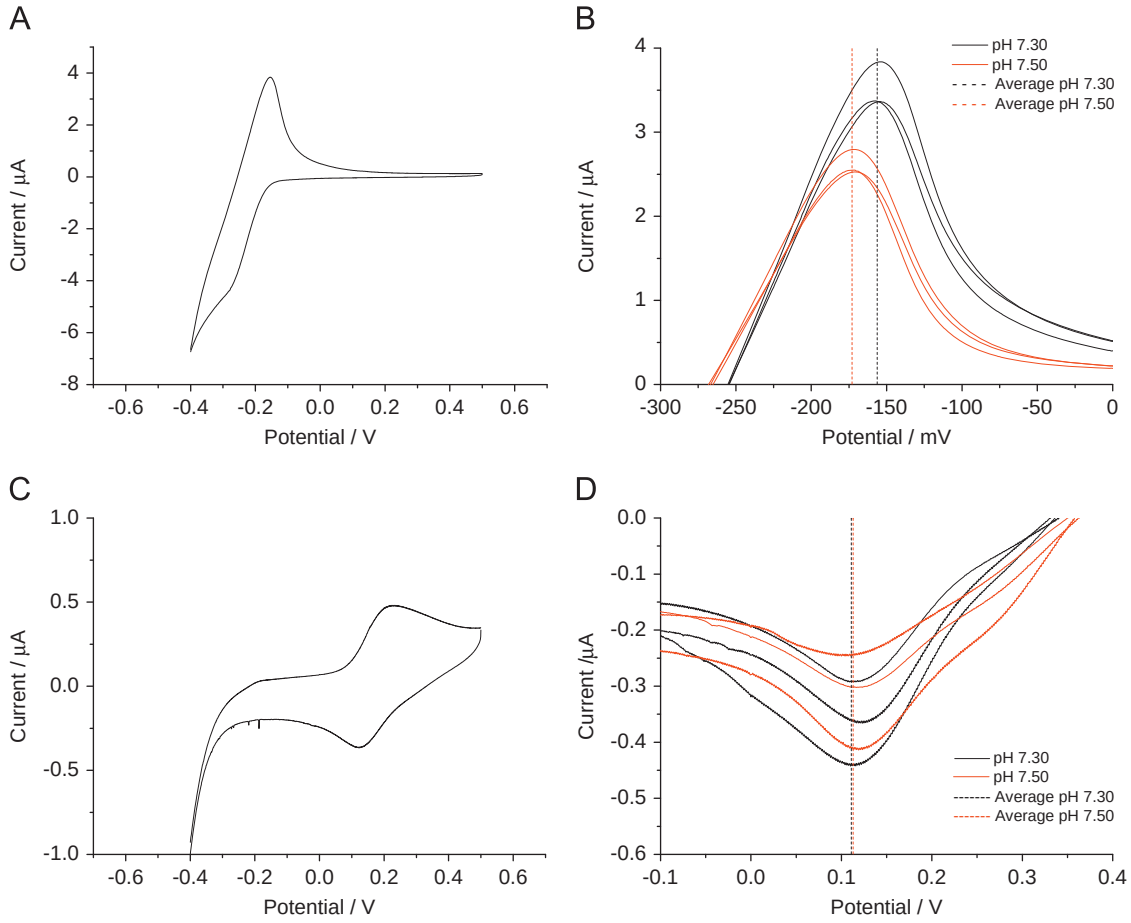

Fig. 3. (A) Typical cyclic voltammogram ($\upsilon = 100$ mV s^{-1}) of a PAQ incorporated sensor in a pH 7.30 buffer solution. (B) Zoom on the anodic peak region (three sensors were characterized at pH 7.30 and pH 7.50). The sensors were characterized against a commercial Ag/AgCl DJRE and a commercial Pt CE. (C) Typical cyclic voltammogram ($\upsilon = 100$ mV s^{-1}) of a Fc incorporated sensor in pH 7.30 buffer solution. (D) Zoom on the cathodic peak region (three sensors were characterized at pH 7.30 and pH 7.50). The sensors were characterized against a commercial Ag/AgCl DJRE and a commercial Pt CE.

revealing the presence of a cathodic peak (Fig. 3A). This confirmed the presence of the redox couple Q/QH_2.

From cyclic voltammograms taken in two different pH buffer solutions, a clear shift of the anodic peak towards more negative potentials is noticed: the average potential of the peak at pH 7.30 and pH 7.50 was -155 ± 2 mV and 171 ± 2 mV ($n = 3$ samples), respectively (Fig. 3B). This change in potential corresponds to a sensor sensitivity of approximately 84 mV/pH. This response was greater than the theoretically predicted Nernstian response and is also referred to as "Super Nernstian". Such a behavior was already observed in other works, but the details of its origin still require further investigation [34]. While the theoretical Nernstian response is obtained and well understood for dissolved redox species, here the species were incorporated into the electrode matrix and might involve other side processes that result in a slightly different sensor sensitivity.

The cyclic voltammograms of the electrodes incorporating Fc molecules showed both anodic and cathodic peaks revealing the presence of the Fc/Fc+ redox couple (Fig. 3C). Unexpectedly, when increasing the pH of the test solution, the anodic peak shifted towards more positive potentials while it ought to be pH-insensitive and thus stay at a constant position. The average potential of the peak at pH 7.30 and pH 7.50 was 220 ± 8 and 286 ± 4 mV ($n = 3$ samples), respectively. However, the cathodic peak kept the same position and did not shift with pH: the average potential of the peak at pH 7.30 and pH 7.50 was 110 ± 4 mV and 111 ± 12 mV, respectively (Fig. 3D).

Sensors incorporating both PAQ and Fc components were also fabricated and characterized. The cyclic voltammograms of these electrodes revealed the combined presence of the Q/QH_2 and Fc/Fc^+ redox couples, which was in good agreement with the previous cyclic voltammograms obtained for the sensors incorporating each individual compound. Moreover, a pH change of 0.2 units in the test sample involved a similar sensor response (i.e., shift in oxidation peak potential of Q/QH_2 of 16 mV) as previously observed for the sensor incorporating only the PAQ component. Also in agreement with what was previously observed, the oxidation peak of Fc shifted towards more positive potentials, whereas its reduction peak did not. Thus, it was clear that the difference in peak potential between the PAQ oxidation peak and the Fc reduction peak could be used for pH sensing.

Sensors made of similar electrochemical components to the ones used here have been previously reported as able to simultaneously sense proton and oxygen levels [34] and in some cases, they even also showed to function as sulfide sensors. In our opinion these characteristics could be taken as advantages for the final sensors, and simultaneous detection of several components. Nevertheless, it was considered beyond the scope of this paper to further investigate these properties.

3.3. pH monitoring

3.3.1. Cyclic voltammetry experiments

After confirming the working principle of the developed voltammetric sensors, their pH response was investigated in more

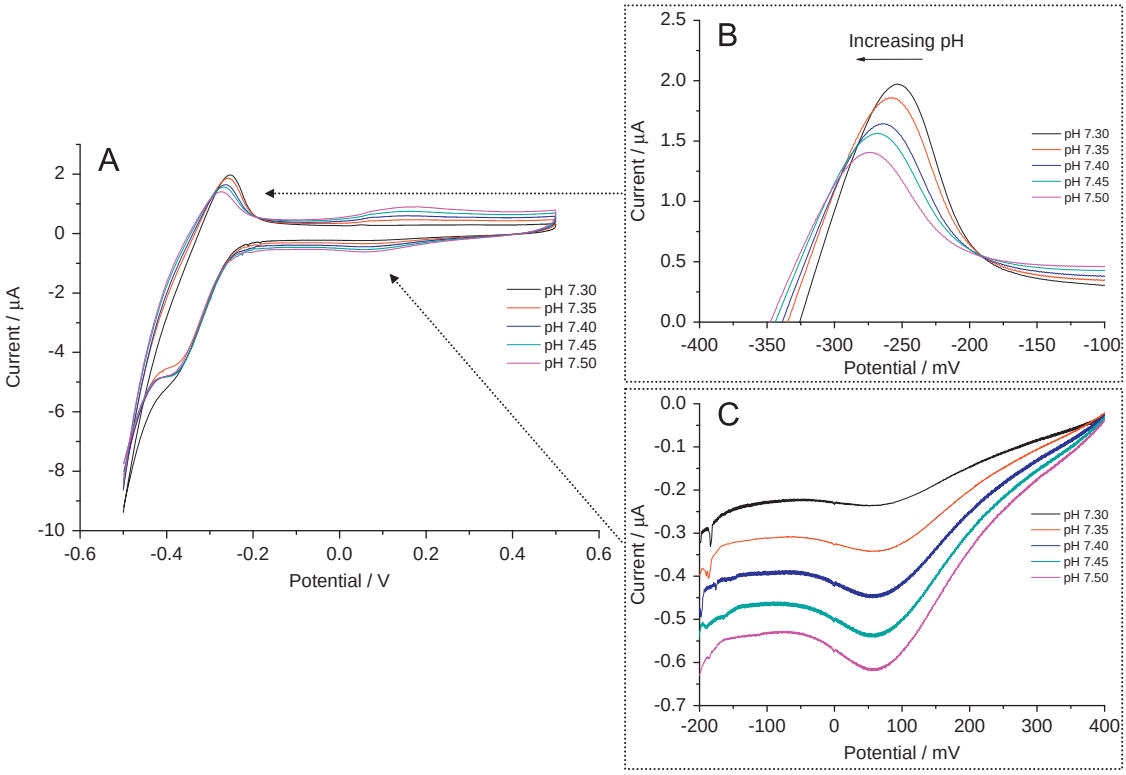

Fig. 4. (A) Typical cyclic voltammograms ($\upsilon = 100$ mV s^{-1}) in various pH buffers of a PAQ/Fc incorporated sensor versus an Ag/AgCl QRE. B. Zoom on the anodic peak region of the PAQ. (C) Zoom in the cathodic peak region of Fc.

detail. Here, the system "on chip sensing electrode versus Ag/AgCl QRE" was characterized. As seen in Fig. 4, the cyclic voltammograms obtained displayed the identical shape as the ones previously obtained when characterizing the sensors versus a commercial DJRE.

In accordance with the previous results, the response to pH of the PAQ compound and the "insensitivity to pH" of the Fc compound were both confirmed (Fig. 4B and C).

In addition, the voltammetric response of three PAQ/Fc incorporated electrodes was verified in order to evaluate the reproducibility of the sensors. In Fig. 5, the peak potentials of PAQ (anodic peak) and Fc (cathodic peak) as well as the potential difference between these two are displayed at each pH value investigated. From this series of experiments, the pH response of PAQ was on average -89.6 mV/pH whereas taking the peak difference between the PAQ oxidation peaks and the Fc reduction peaks resulted in an average pH sensitivity of -97.0 mV/pH. These two responses were greater than the one predicted by the Nernstian equation and thus also denoted as "Super Nernstian". This type of response was also observed by Lafitte et al. [34] and is still not fully understood.

Taking into account the manual fabrication of the sensors, the reproducibility of the experiments (from sensor to sensor) was good. This was highlighted by typical error values of less than 3 mV for the PAQ peaks and 4.5 mV for the peak difference values ($n=3$ samples), which is in good agreement with the values obtained in previous works ([25] and the cited references).

Moreover, for the last series of CV experiments the sensors to be characterized were used 9 days after the first electrochemical experiments (meanwhile, the sensors were stored dry) and still displayed an unaffected voltammetric response. This proved the confinement of the PAQ and Fc compounds in the graphite electrodes and also highlighted the good lifetime of sensors despite the very simple physical incorporation technique used. Identical results were previously obtained by Heald et al. [41] using a much more complex chemical derivatization method of carbon nanotubes to incorporate the electroactive species on the sensors.

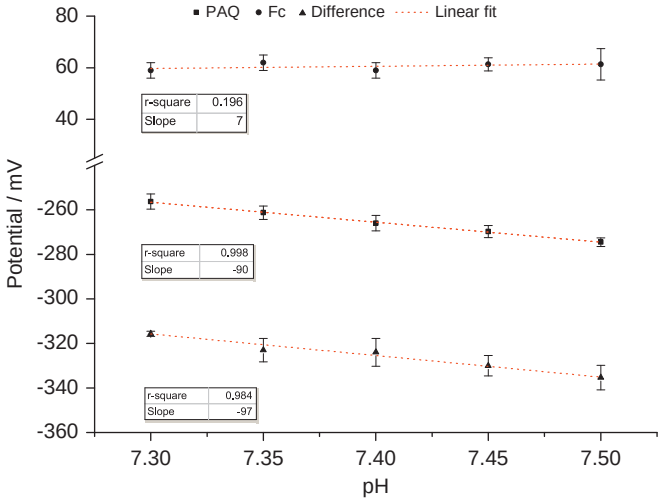

Fig. 5. Plot of the peak potential against pH for PAQ (■), Fc (●) and the difference between the two (▲) ($n=3$ samples).

3.3.2. *Square-wave voltammetry experiments*

SWV was then used as a means to obtain sharper and well defined voltammetric peaks in single sweep experiments [41].

Contrary to our expectations, the square-wave voltammograms obtained for the PAQ/Fc incorporated sensors displayed fairly broad peaks. Further investigation of the influence of experimental parameters such as the frequency, potential step and amplitude did not improve the sharpness of the peaks. Even

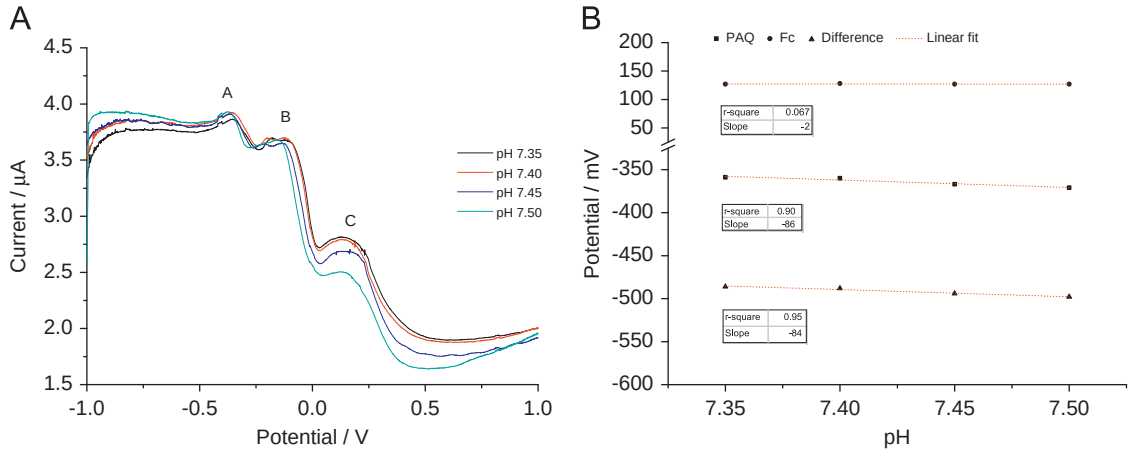

Fig. 6. (A) Typical square-wave voltammetric response in various pH buffer solutions of a PAQ/Fc incorporated sensor versus a DJRE. (B) Typical peak potential variation of PAQ (■), Fc (●) and the difference between the two (▲) in various pH buffer solutions (Peaks A, B, and C are described in the text).

changing the contents of the sensor paste (PAQ/Fc ratio in the graphite matrix) was attempted without any significant improvement of the signal sharpness.

Typical square-wave voltammetric curves carried out on a PAQ/Fc incorporated sensor versus a DJRE and a Pt CE are displayed in Fig. 6A.

Despite the relatively broad shape of the obtained peaks, it was possible to identify the peak responsible for the presence of PAQ (at $E\sim-0.361$ V in a pH 7.30 buffer solution, Fig. 6A, peak A) and the peak responsible for the presence of Fc (at $E\sim0.127$ V in all pH buffer solutions, Fig. 6A, peak C).

From square-wave voltammograms taken in various pH solutions, the response to pH of the PAQ compound was −86.0 mV/pH and thus lower but still in fairly good agreement with the previous results from the CV experiments. Moreover, the redox wave of the Fc compound only slightly shifted towards negative potential with increasing pH and could therefore be used as internal reference. As a result, a pH response of −84.0 mV/pH was obtained for the PAQ compound with respect to Fc. Fig. 6B summarizes the influence of pH on the redox peak position of the different electroactive species as well as the difference between the two peaks.

In the square-wave voltammograms, a third peak centered on $E\sim0.150$ V was also observed (see peak B in Fig. 6A). This peak was not very pronounced for some of the experiments (especially for square-wave voltammogram frequencies above 25 Hz) and did not display any clear or significant correlation between its position and pH. A double peak in the square-wave voltammograms was also previously observed in other works [35,42] for similar compounds and tentatively attributed to the redox chemistry of PAQ. However, this phenomenon was typically seen at high pH (i.e., above pH 12). In [42], the shoulder in the peak currents was attributed to the reduction of quinone to semi-quinone species.

4. Conclusions

The fabrication process used to manually screen-print graphite electrodes has proven to stand for a fast, inexpensive and relatively reproducible fabrication method for the development of electrochemical systems. The fabricated graphite based sensors displayed electrochemical properties very close to the ones of semi-automatically fabricated sensors. This method represents a much simpler way to incorporate electroactive redox components (i.e., PAQ as a pH-sensitive species and Fc as a pH-insensitive species) into graphite electrodes compared to other techniques such as covalent chemical derivatization on carbon materials with electroactive species [41,42]. Moreover, the fact that the redox species were incorporated into the electrodes and not immobilized on them presented the advantage of avoiding fast depletion of the species from the electrodes, which could shorten the lifetime of the sensors. Some of the developed sensors were actually stored in dry environment during nine days between two electrochemical experiments and still displayed very good properties, attesting to their good lifetime despite their simple fabrication.

Another major advantage of this type of sensors featuring both sensing and reference species was that the difference between the redox peaks of the two species was taking into account. Therefore, potential drift of the reference half-cell was not as detrimental as for common three electrode electrochemical setups, and the use of a simple QRE was permitted.

The CV experiments showed the clear presence of the PAQ and Fc redox couples incorporated in the sensors. On the one hand, the oxidation peak for PAQ shifted as expected towards more negative potentials with increasing pH and thus validated the implementation of PAQ as the pH-sensitive species. On the other hand, the oxidation peak for Fc also shifted with pH; however, its reduction peak did not. Thus, the use of Fc as a pH-insensitive species or internal reference species was also confirmed.

Recording the position of the oxidation peak of PAQ with respect to the reduction peak of Fc was successfully used for pH monitoring and resulted in a super Nernstian pH-response of −97.0 mV/pH. This type of response was also observed earlier by Lafitte et al. [34] for identical components and remains not yet fully understood.

The SWV experiments resulted in voltammograms with redox peaks broader than expected. However, the response of the sensors remained fairly identical to the one obtained from the cyclic voltammograms.

Thus, the electrochemical voltammetric sensors displayed very good pH-response, potential stability and reproducibility in test buffers. In this paper, emphasis was put on the description of the simplicity and usefulness of the concept and fabrication technique of voltammetric sensors featuring both indicator and reference species, however, additional experiments will also need to be carried out to investigate the behavior of the sensors in real physiological samples.

The simplicity of the incorporation method used here could allow the development of electrochemical system implementing

several indicator molecules in the sensor paste for parallel detection of other components.

Acknowledgments

The authors would like to acknowledge Radiometer Medical for financial support.

References

[1] H. Nam, G.S. Cha, T.D. Strong, J. Ha, J.H. Sim, R.W. Hower, S.M. Martin, R.B. Brown, Proc. IEEE 91 (6) (2003) 870–880.
[2] H. Suzuki, A. Hiratsuka, S. Sasaki, I. Karube, Sens. Actuators B 46 (2) (1998) 104–113.
[3] H. Suzuki, T. Hirakawa, S. Sasaki, I. Karube, Sens. Actuators B 46 (22) (1998) 5069–5075.
[4] H.J. Yoon, J.H. Shin, S.D. Lee, H. Nam, G.S. Cha, T.D. Strong, R.B. Brown, Sens. Actuators B 64 (1–3) (2000) 8–14.
[5] A. Simonis, H. Lüth, J. Wang, M.J. Schöning, Sens. Actuators B 103 (1–2) (2004) 429–435.
[6] J. Ha, S.M. Martin, Y. Jeon, I.J. Yoon, R.B. Brown, H. Nam, G.S. Cha, Anal. Chim. Acta 549 (1–2) (2005) 59–66.
[7] A.W.J. Cranny, J.K. Atkinson, Meas. Sci. Technol. 9 (9) (1998) 1557–1565.
[8] Ł. Tymecki, E. Zwierkowska, R. Koncki, Anal. Chim. Acta 526 (1) (2004) 3–11.
[9] J.K. Atkinson, M. Glanc, P. Boltryk, M. Sophocleous, E. Garcia-Breijo, Microelectron. Int. 28 (2) (2011) 49–52.
[10] H. Jahn, H. Kaden, Microchim. Acta 146 (2) (2004) 173–180.
[11] J. Ghilane, P. Hapiot, A.J. Bard, Anal. Chem. 78 (19) (2006) 6868–6872.
[12] N.H. Kwon, K.S. Lee, M.S. Won, Y.B. Shim, Analyst 132 (9) (2007) 906–912.
[13] A. Kisiel, A. Michalska, K. Maksymiuk, E.A.H. Hall, Electroanalysis 20 (3) (2008) 318–323.
[14] Y.H. Liao, J.C. Chou, J. Electrochem. Soc. 155 (10) (2008) 257–262.
[15] C.C. Chen, J.C. Chou, Jpn. J. Appl. Phys. 48 (11) (2009) 111501.
[16] J. Zhou, K. Ren, Y. Zheng, J. Su, Y. Zhao, D. Ryan, H. Wu, Electrophoresis 31 (18) (2010) 3083–3089.
[17] W. Vonau, W. Oelßner, U. Guth, J. Henze, Sens. Actuators B 144 (2) (2010) 368–373.
[18] A. Kisiel, M. Donten, J. Mieczkowski, F.X. Rius-Ruiz, K. Maksymiuk, A. Michalska, Analyst 135 (9) (2010) 2420–2425.
[19] J. Gabel, W. Vonau, P. Shuk, U. Guth, Solid State Ionics 169 (1–4) (2004) 75–80.
[20] U. Guth, F. Gerlach, M. Decker, W. Oelßner, W. Vonau, J. Solid State Electrochem. 13 (1) (2009) 27–39.
[21] M.W. Shinwari, D. Zhitomirsky, I.A. Deen, P.R. Selvaganapathy, M.J. Deen, D. Landheer, Sensors 10 (3) (2010) 1679–1715.
[22] H. Suzuki, Electroanalysis 12 (9) (2000) 703–715.
[23] R.P. Buck, E. Lindner, Anal. Chem. 73 (3) (2001) 88–97.
[24] J.J. Hickman, D. Ofer, P.E. Laibinis, G.M. Whitesides, M.S. Wrighton, Science 252 (5006) (1991) 688–691.
[25] D.K. Kampouris, R.O. Kadara, N. Jenkinson, C.E. Banks, Anal. Methods 1 (2009) 25–28.
[26] Ł. Tymecki, S. Glab, R. Koncki, Sensors 6 (2006) 390–396.
[27] M. Prudenziati, B. Morten, Microelectron. J. 23 (2) (1992) 133–141.
[28] C.A.Galán Vidal, J. Munoz, C. Dominguez, S. Alegret, Trends Anal. Chem. 14 (5) (1995) 225–231.
[29] S. Laschi, I. Palchetti, G. Marrazza, M. Mascini, J. Electroanal. Chem. 593 (2006) 211–218.
[30] O.Domínguez Renedo, M.A. Alonso-Lomillo, M.J.Arcos Martínez, Talanta 73 (2) (2007) 202–219.
[31] J.P. Hart, S.A. Wring, Trends Anal. Chem. 16 (2) (1997) 89–103.
[32] M. Tudorache, C. Bala, Anal. Bioanal. Chem. 388 (2007) 565–578.
[33] R.O. Kadara, N. Jenkinson, C.E. Banks, Sens. Actuators B 138 (2009) 556–562.
[34] V.G.H. Lafitte, W. Wang, A.S. Yashina, N.S. Lawrence, Electrochem. Commun. 10 (2008) 1831–1834.
[35] N.S. Lawrence, M. Pagels, S.F.J. Hackett, S. McCormack, A. Meredith, T.G.J. Jones, G.G. Wildgoose, R.G. Compton, L. Jiang, Electroanalysis 19 (4) (2006) 424–428.
[36] C.R. Friedrich, P.J. Coane, M.J. Vasile, Microelectron. Eng. 35 (1–4) (1997) 367–372.
[37] C.G. Khan Malek, Anal. Bioanal. Chem. 385 (8) (2006) 1362–1369.
[38] C.G. Khan Malek, Anal. Bioanal. Chem. 385 (8) (2006) 1351–1361.
[39] A.E. Musa, Development of Miniaturized Disposable Electrochemical Systems Intended for Point of Care Blood Analysis, Ph.D. Thesis, Technical University of Denmark, DTU Nanotech, Kongens Lyngby, 2011, ISBN:978-87-91797-40-8.
[40] V.D. Parker, in: A.J. Bard (Ed.), Electroanalytical Chemistry, vol. 14, Dekker, New York, 1986.
[41] C.G.R. Heald, G.G. Wildgoose, L. Jiang, T.G.J. Jones, R.G. Compton, Chem. Phys. Chem. 5 (11) (2004) 1794–1799.
[42] G.G. Wildgoose, M. Pandurangappa, N.S. Lawrence, L. Jiang, T.G.J. Jones, R.G. Compton, Talanta 60 (5) (2003) 887–893.